Isomerization of Dihydrobenzofuran and Isodihydrobenzofuran. Quantum Chemical and Kinetics Calculations

Faina Dubnikova and Assa Lifshitz*

Department of Physical Chemistry, The Hebrew University, Jerusalem 91904, Israel

Received: June 5, 2002; In Final Form: July 30, 2002

The isomerizations of dihydrobenzofuran and isodihydrobenzofuran were studied by the Becke three-parameter hybrid method with Lee−Yang−Parr correlation functional approximation (B3LYP). Structure and frequency calculations were carried out with the Dunning correlation-consistent polarized double ξ (cc-pVDZ) and augmented aug-cc-pVDZ basis sets. The energetics was calculated using coupled cluster theory CCSD(T). Both reactions proceed via stepwise mechanisms. The potential energy surface of the dihydrobenzofuran → *o*-hydroxystyrene isomerization has one intermediate and two transition states. In the isodihydrobenzofuran → *o*-tolualdehyde isomerization, there are two intermediates and three transition states on the surface. Whereas a stable intermediate is produced in the dihydrobenzofuran isomerization, the intermediates in isodihydrobenzofuran are unstable biradicals. The last step in both isomerizations is a H-atom migration. The intermediate that is formed in dihydrobenzofuran isomerization, methyl-2-methylene-3,5-cyclohexadiene-1-one, is very stable despite the complete loss of resonance energy of the benzene ring. This was proven to be due to the formation of a very strong >C═O bond in the process. Rate constants based on the quantum chemical calculations using transition-state theory are in very good agreement with the experimental results.

I. Introduction

Heterocyclic compounds fused to aromatic rings are the most common compounds containing oxygen and nitrogen in coal, petroleum, and other nonpetroleum fuels.[1] The presence of the benzene ring stabilizes the fused ring compounds.[2−4] Reaction channels that destroy the resonance energy of the benzene ring are considered to be slow in the fused ring compound compared to their rates in the single ring. Dihydrobenzofuran and isodihydrobenzofuran are two structural isomers that differ from one another in the location of the oxygen atom with respect to the benzene ring.

In these two molecules, the fused benzene ring replaces the C═C double bond in 2,3-dihydrofuran and 2,5-dihydrofuran.

The isomerization products of 2,3-dihydrofuran are propenyl aldehyde and cyclopropanecarboxaldehyde,[5]

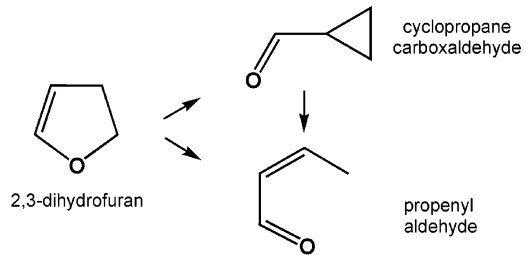

whereas, the main reaction of dihydrobenzofuran is isomerization to *o*-hydroxystyrene.[6]

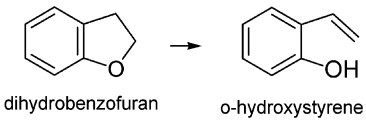

The species that may be considered similar to the three-membered ring compound, cyclopropanecarboxaldehyde, which is is formed in the isomerization of 2,3-dihydrofuran, is unstable when the furan ring is fused to benzene and is not formed in the thermal reactions of dihydrobenzofuran.

Isodihydrobenzofuran undergoes isomerization to *o*-tolualdehyde as the main thermal reaction,[7] whereas in 2,5-dihydrofuran the main reaction is H_2 elimination to form furan.[8−10]

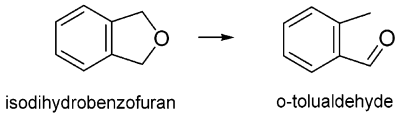

We present in this article quantum chemical calculations of the reaction pathways of the isomerization of these compounds and compare the calculations with the experimental results obtained with the single pulse shock tube technique.

II. Computational Details

We used the Becke three-parameter hybrid method[11] with Lee−Yang−Parr correlation functional approximation (B3LYP)[12] and the Dunning correlation-consistent polarized valence double ξ (cc-pVDZ) basis set.[13] Structure optimization of the reactants and products was done using the Berny geometry optimization algorithm.[14] For determining transition-state structures, we used

10.1021/jp0213396 CCC: $22.00
Published on Web 09/17/2002

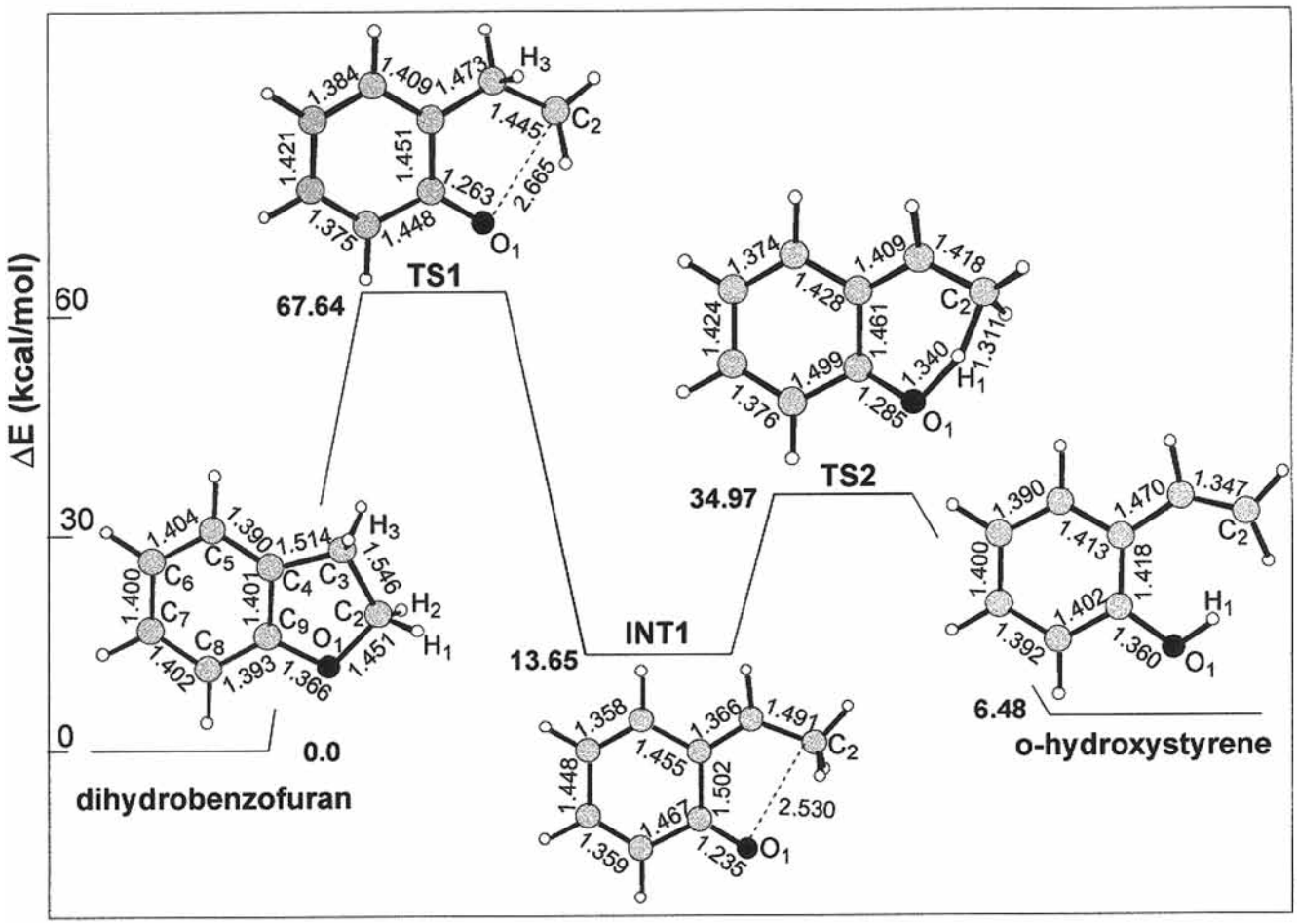

Figure 1. Reaction pathway for dihydrobenzofuran → *o*-hydroxystyrene isomerization. Relative energies (in kcal/mol) are calculated at CCSD-(T)//B3LYP/cc-pVDZ level of theory. Bond distances are given in Å units.

the combined synchronous transit-guided quasi-Newton (STQN) method.[15] The higher-level calculations were done using these geometries.

All of the calculations were performed without symmetry restrictions**.** Vibrational analyses were done at the same level of theory to characterize the optimized structures as local minima or transition states. Calculated vibrational frequencies and entropies (at B3LYP level) were used to evaluate preexponential factors of the reactions under consideration**.** All of the calculated frequencies, the zero-point energies, and the thermal energies are of harmonic oscillators. The calculations of the intrinsic reaction coordinate (IRC) to check whether the transition states under consideration connect the expected reactants and products were done at the B3LYP level of theory with the same basis set as was used for the stationary-point optimization**.** These calculations were done on all of the transition states.

The points on the potential energy surfaces having a biradical character were located by the unrestricted uB3LYP method using guess wave function with the destructive $\alpha-\beta$ and spatial symmetry. We used an open-shell singlet approximation for the biradical structures. It should be mentioned that numerous recent studies indicate that the spin-unrestricted B3LYP method for geometry optimization of biradical transition states and intermediates and for energy barriers on the surface was in a reasonable agreement with the results of the multireference or multiconfigurational calculations and the corresponding experimental data.[18−20]

We have examined the multireference character of the transition states and intermediates by determining their T_1 value, which according to a diagnostic that was introduced by Lee and Taylor reflects the extent of the multireference character of the species on the surface.[19] In some species, the T_1 values were considerably higher than 0.02, a value that is being considered as the highest value below which the multireference character is negligible.[20] However, it has been shown[21−23] that the coupled cluster method, with the inclusion of estimates for the effects of triple excitations, can compensate for inadequacies in the single-determinant reference. In view of these findings, we used the coupled cluster theory CCSD(T) for configuration interaction calculations at B3LYP geometry. CCSD(T) calculations were performed with the frozen-core approximation. All of the reported relative energies include zero-point energy correction (ZPE).

The DFT and CCSD(T) computations were carried out using the Gaussian 98 program package[24] and were done on a DEC Alpha XP1000 1/667 professional workstation.

III. Results of the Quantum Chemical Calculations

A. Dihydrobenzofuran → *o*-Hydroxystyrene Isomerization. The potential energy surface of dihydrobenzofuran → *o*-hydroxystyrene isomerization and selected structural parameters of the species on the surface are shown in Figure 1. The energetics and other parameters relevant to this surface are shown in Table 1. The surface contains two transition states and one intermediate.

TABLE 1: Total Energies, E_{total} (in au), Zero-Point Energies, Relative Energies, ΔE,[a] Imaginary Frequencies,[b] and Entropies[c] for All of the Species on the Dihydrobenzofuran Isomerization Surface, Calculated at B3LYP/cc-pVDZ and CCSD(T)/cc-pVDZ//B3LYP/cc-pVDZ Levels of Theory

	B3LYP					CCSD(T)	
species	E_{total}	ΔE^a	ZPE	S^c	ν^b	E_{total}	ΔE^a
dihydrobenzofuran	−384.905 301	0.00	87.77	81.45		−383.827 342	0.0
TS1	−384.791 814	66.10	82.66	85.01	(i-450)	−383.711 407	67.64
INT1	−384.879 070	14.24	85.55	87.68		−383.802 050	13.65
TS2	−384.851 393	29.30	83.24	81.67	(i-1567)	−383.764 390	34.97
o-hydroxystyrene	−384.893 599	6.02	86.45	85.08		−383.814 970	6.48

[a] Relative energies in kcal/mol. $\Delta E = \Delta E_{total} + \Delta(ZPE)$. [b] Imaginary frequencies in cm^{-1}. [c] Entropies in cal/(K mol).

The surface of the similar process in 2,3-dihydrofuran → propenyl aldehyde isomerization,

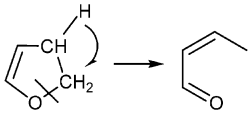

contains only one transition state and no intermediates.[25] However, the transition state in this isomerization is very similar to the first transition state in the dihydrobenzofuran → *o*-hydroxystyrene isomerization toward the formation of **INT1**. **INT1**, methyl-2-methylene-3,5-cyclohexadiene-1-one, has a carbonyl group similar to the one in propenyl aldehyde, $CH_3CHCHCHO$, which is the product of 2,3-dihydrobenzofuran isomerization. The formation of propenyl aldehyde in the above-mentioned process, as well as methyl-2-methylene-3,5-cyclohexadiene-1-one during the dihydrobenzofuran isomerization, are concerted processes in which the rupture of the O(1)−C(2) bond and the H-atom migration from C(3) to C(2) occur simultaneously (see Figure 1). The reaction coordinate in the transition state **TS1** is H-atom migration from C(3) to C(2) and a simultaneous rotation of the methylene group C(2)H(1)H(2) with respect to the O(1)C(9)C(4) plane. Because of the C(2)H(1)H(2) methylene group rotation, the O(1)−C(2) bond distance increases from 1.451 to 2.665 Å. The bond length of C(3)−H(3) increases from 1.095 to 1.152 Å simultaneously with a dramatic change of the H(3)C(3)C(2) angle, which varies from 111.15° in dihydrobenzofuran to 85.37° in **TS1**. It also brings H(3) closer to C(2) to form the new C(2)−H(3) bond in **INT1**. The result of the O(1)−C(2) bond breaking is shortening of the O(1)−C(9) bond from a single bond (1.366 Å) to almost a double bond (1.263 Å) in the transition state. The aromaticity of the fused benzene ring is destroyed in this process.

The energy barrier of this stage is 67.64 kcal/mol at CCSD(T)//B3LYP/cc-pVDZ level of theory, and it is the highest barrier on the potential energy surface. This barrier is slightly higher than the corresponding barrier in the 2,3-dihydrofuran isomerization.

The energy level of **INT1** (methyl-2-methylene-3,5-cyclohexadiene-1-one) relative to dihydrobenzofuran is +13.65 kcal/mol at CCSD(T)//B3LYP/cc-pVDZ level of theory (Figure 1). This relatively small difference came as somewhat of a surprise to us because the resonance of the benzene ring in **INT1** is completely lost.

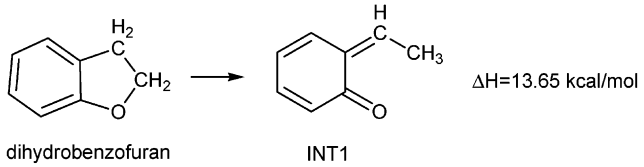

To examine whether this loss of resonance is compensated by the strong >C═O bond in methyl-2-methylene-3,5-cyclohexadiene-1-one, we calculated, for comparison, the energetics of the equivalent path: dihydroindene → methyl-2-methylene-3,5-cyclohexadiene-1-methylene (virtual **INT1**):

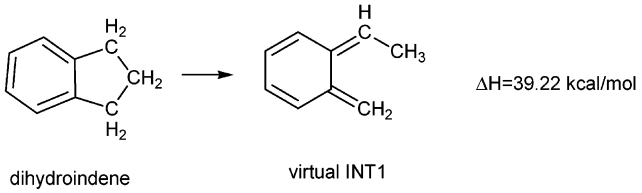

The loss of resonance of the benzene ring in this path is very well established in the calculations. The difference in the stability of the two intermediates relative to their origin is ∼25.5 kcal/mol at CCSD(T)//B3LYP/cc-pVDZ level of theory. This difference results from the difference between the bond strength of >C═O and >C═CH_2 in the two intermediates. One can reach the conclusion that the loss of resonance of the benzene ring going from dihydrobenzofuran to **INT1** is indeed compensated to a large extent by the formation of a strong >C═O bond. Considering also the fact that an intramolecular H-bond between O(1) and the hydrogen atoms of the methyl group, estimated as >5 kcal/mol, does exist in methyl-2-methylene-3,5-cyclohexadiene-1-one (**INT1**), its increased stability is even higher.

It is interesting to note that quinones are stable organic molecules that can be obtained from the shelf, whereas 3,6-dimethylene-1,4-cyclohexadiene does not exist as a stable compound.

The second step of the dihydrobenzofuran isomerization is an oxo ⇔ hydroxy tautomerization, where methyl-2-methylene-3,5-cyclohexadiene-1-one forms *o*-hydroxystyrene. This step proceeds with a low barrier of ∼21 kcal/mol. The reaction coordinate in this step is a 1,5-H-atom migration from C(2) to O(1) via transition state **TS2**, which has a structure similar to a six-membered ring fused to benzene. The main change in this structure going from the intermediate **INT1** to the transition state **TS2** is a decrease in the H(1)−O(1) distance and an increase in the H(1)−C(2) distance toward the formation of an alcohol from the ketone. They change from 2.53 to 1.34 Å and from 1.103 to 1.311 Å, respectively.

B. Isodihydrobenzofuran → *o*-Tolualdehyde Isomerization. The potential energy surface of isodihydrobenzofuran → *o*-tolualdehyde isomerization is shown in Figure 2. All of the intermediates and transition states on the surface have open-shell structures. The figure contains selected structural parameters of the species on the surface and the location of the high electron density (●). The energetics both at uB3LYP/cc-pVDZ and at uCCSD(T)//uB3LYP/cc-pVDZ levels of theory is shown in Table 2.

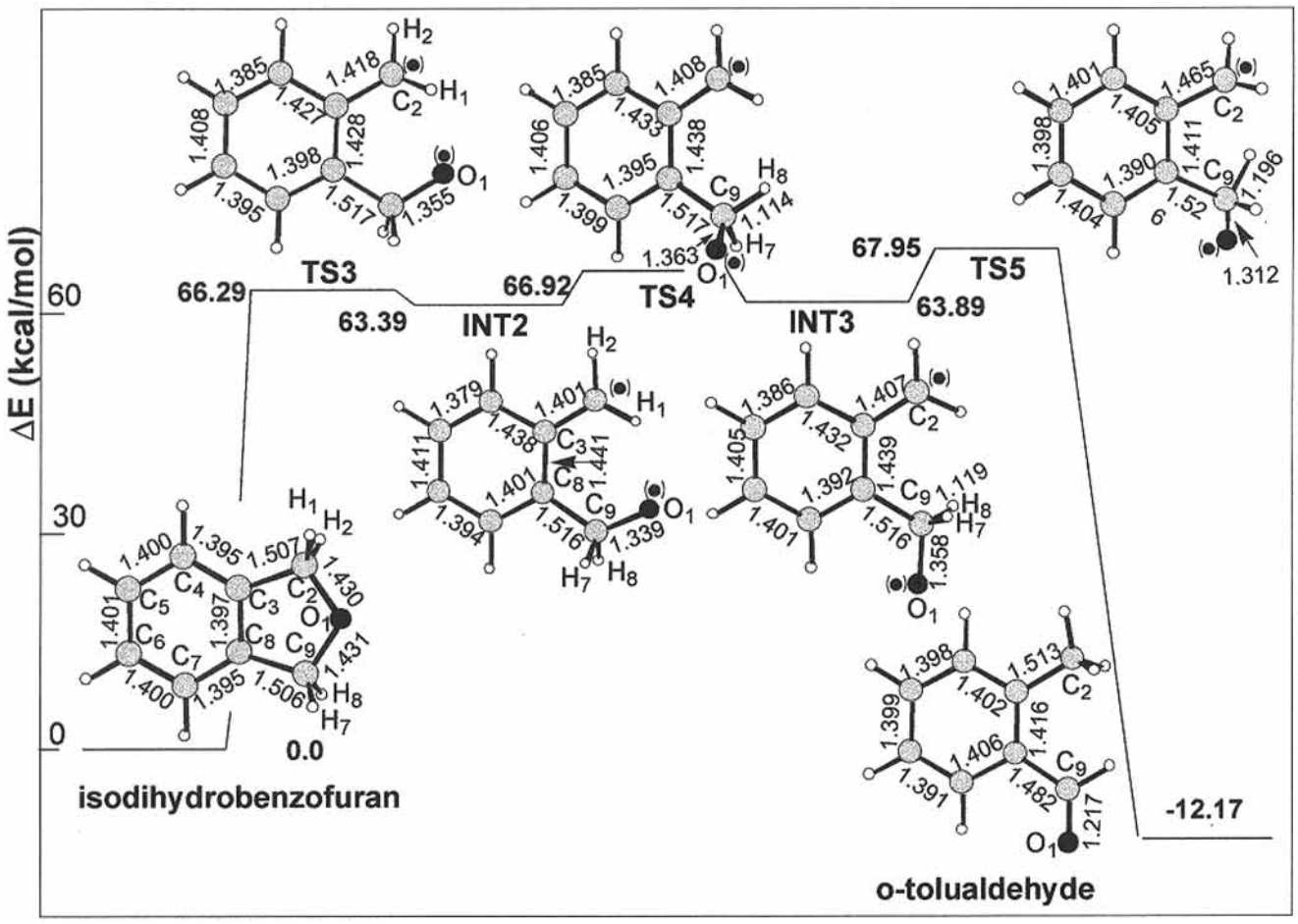

Figure 2. Reaction pathway for isodihydrobenzofuran → *o*-tolualdehyde isomerization. Relative energies (in kcal/mol) are calculated at uCCSD(T)//uB3LYP/cc-pVDZ level of theory. Bond distances are given in Å units. The symbol (●) denotes partially distributed free electron density.

TABLE 2: Total Energies, E_{total} (in au), Zero-Point Energies, Relative Energies, ΔE,[a] Imaginary Frequencies,[b] Entropies,[c] and Spin Contamination for All of the Species on the Isodihydrobenzofuran Isomerization Surface, Calculated at B3LYP/cc-pVDZ and CCSD(T)/cc-pVDZ//B3LYP/cc-pVDZ Levels of Theory

	uB3LYP						uCCSD(T)	
species	E_{total}	ΔE^a	ZPE	S^c	ν^b	$\langle S^2 \rangle$	E_{total}	ΔE^a
isodihydrobenzofuran	−384.895 913	0.00	87.46	83.01		0.0	−383.818 194	0.0
TS3	−384.792 907	60.51	83.64	83.43	(i-330)	0.5435	−383.706 464	66.29
INT2	−384.797 112	57.63	83.09	87.17		0.7627	−383.697 481	63.39
TS4	−384.789 936	61.65	82.61	84.71	(i-102)	0.9894	−383.703 815	66.92
INT3	−384.795 449	58.57	82.99	87.09		1.0192	−383.709 254	63.89
TS5	−384.774 833	70.05	81.53	84.54	(i-756)	0.7288	−383.700 457	67.95
o-tolulaldehyde	−384.910 419	−10.50	86.06	87.06		0.0	−383.835 353	−12.17

[a] Relative energies in kcal/mol. $\Delta E = \Delta E_{total} + \Delta(ZPE)$. [b] Imaginary frequencies in cm^{-1}. [c] Entropies in cal/(K mol).

The isomerizations in both dihydrobenzofuran and isodihydrobenzofuran involve the opening of the five-membered ring via C−O bond cleavage followed by H-atom migration. In dihydrobenzofuran, the H-atom migrates from a carbon to its neighboring oxygen atom. However, in isodihydrobenzofuran, the migration takes place between two carbon atoms that are further apart. To facilitate the migration, the distance between the migrating hydrogen atom and the receiving carbon atom must be shortened. This requires an additional step that involves rotation of the C(9)H(7)H(8) methylene group with respect to the benzene ring. The isodihydrobenzofuran surface contains, therefore, an additional transition state and intermediate. The two intermediates that can be found in the surface differ from one another by the orientation of the $O-CH_2$ group with respect to the benzene ring. The energies of the two intermediates are the same.

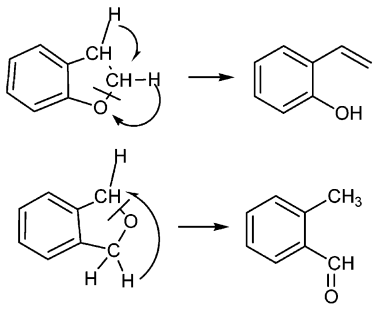

In contrast to the dihydrobenzofuran surface, the result of the bond-breaking step (first step) in isodihydrobenzofuran is

an unstable biradical intermediate because no rearrangement in the intermediate takes place following the bond breaking. The reaction coordinate in the bond-breaking process is O(1)−C(2) bond stretch combined with C(2)H(1)H(2) methylene group rotation relative to the benzene plane. The energy barrier of this stage (the O−C bond breaking) is 66.29 kcal/mol.

The second step on the potential energy surface is the aforementioned rotation with a small barrier of ∼3.5 kcal/mol. The dihedral angle O(1)C(9)C(8)C(3) changes from 11° in **INT2** to 180° in **INT3**. The angle in **TS2** is 113°. The imaginary frequency associated with this reaction coordinate is rather low, 102 cm^{-1}.

The last step of the isodihydrobenzofuran isomerization is a 1,4-H-atom shift from C(9) to C(2). Whereas the reaction coordinate in the equivalent step in dihydrobenzofuran, **INT1** → **TS2** → *o*-hydroxystyrene, is simply 1,5-H-atom shift, the reaction coordinate in isodihydrobenzofuran, **INT3** → **TS5** → *o*-tolualdehyde, involves in addition to a 1,4-H-atom shift also a considerable movement of C(2) and C(9) toward one another. This reflects itself by the decrease in the C(2)−C(9) distance from 2.989 Å in the intermediate **INT3** to 2.682 Å in **TS5**. Note that this bond-distance shortening in the transition state is accompanied (or caused) by a decrease in the bond angles C(2)C(3)C(8) and C(3)C(8)C(9) from ∼123° and ∼121° in the intermediate **INT3** to ∼116° and ∼114° in the transition state, respectively. Note also that the imaginary frequency in **TS2** (dihydrobenzofuran) is 1567 cm^{-1}, whereas in **TS5** (isodihydrobenzofuran) it is only 756 cm^{-1}.

The potential energy surface for isodihydrobenzofuran isomerization from **TS3** to **TS5** is very shallow (Figure 2). The energy level of the transition state **TS5** is the highest on the surface; its value is 67.95 kcal/mol relative to that of isodihydrobenzofuran. This value was used for rate constant calculation as the barrier of the process of isomerization.

IV. Rate Constant Calculations

To evaluate the high-pressure limit first-order rate constants from the quantum chemical calculations, the relation

$$k_\infty = \Gamma(T)\sigma(kT/h)\exp(\Delta S^{\#}/R)\exp(-\Delta H^{\#}/RT) \qquad (1)$$

was used,[26,27] where h is the Planck constant, k is the Boltzmann factor, σ is the degeneracy of the reaction coordinate, $\Delta H^{\#}$ and $\Delta S^{\#}$ are the temperature-dependent enthalpy and entropy of activation, respectively, and $\Gamma(T)$ is the tunneling correction. Because we deal with unimolecular reactions, $\Delta H^{\#} = \Delta E^{\#}$, where $\Delta E^{\#}$ is the energy difference between the transition state and the reactant. $\Delta E^{\#}$ is equal to $\Delta E^{0}_{\text{total}} + \Delta E^{\circ}_{\text{thermal}}$ where $\Delta E^{0}_{\text{total}}$ is obtained by taking the difference between the total energies of the transition state and the reactant and $\Delta E_{\text{thermal}}$ is the difference between the thermal energies of these species.

The tunneling effect, $\Gamma(T)$, was estimated using Wigner's inverted harmonic model,[28] where

$$\Gamma(T) = 1 + \frac{1}{24}\left(\frac{hc\bar{\lambda}^{\#}}{kT}\right)^2 \qquad (2)$$

and $\bar{\lambda}^{\#}$ is the imaginary frequency of the reaction coordinate in cm^{-1}.[29,30]

To transfer k_∞ to the pressure range of the experiments, to which the calculations will be compared, we performed RRKM calculations. The RRKM calculations employed the standard routine,[31] which uses a direct vibrational state count with classical rotation for the transition state. $\langle \Delta E_{\text{down}} \rangle$ was taken as

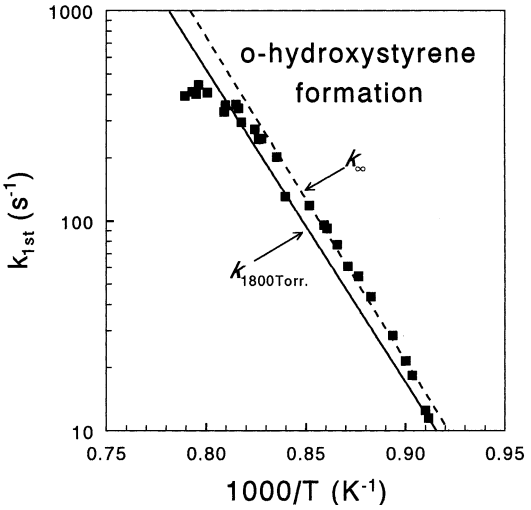

Figure 3. Arrhenius plot of the calculated rate constant of dihydrobenzofuran → *o*-hydroxystyrene isomerization. The solid line corresponds to a pressure of 1800 Torr. The dashed line is k_∞. The two lines include the tunneling corrections. The experimental data are presented as squares on the figure.

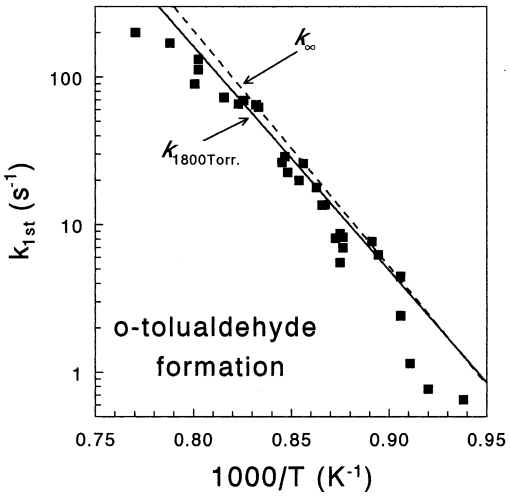

Figure 4. Arrhenius plot of the calculated rate constant of isodihydrobenzofuran → *o*-tolualdehyde isomerization. The solid line corresponds to a pressure of 1800 Torr. The dashed line is k_∞. Tunneling corrections are negligible. The experimental data are presented as squares on the figure.

400 cm^{-1}. The RRKM calculations were carried out at several temperatures, and the values of the rate constants obtained were then plotted as log k vs $1/T$ to obtain the corresponding Arrhenius rate parameters. The values obtained are

$$k_{\text{dihydrobenzofuran}} = 4.54 \times 10^{14}\exp(-68.30 \times 10^3/RT)\ s^{-1}$$

$$k_{\text{isodihydrobenzofuran}} = 2.30 \times 10^{14}\exp(-69.48 \times 10^3/RT)\ s^{-1}$$

where R is expressed in units of kcal/mol. Figures 3 and 4 show a comparison between the calculated Arrhenius rate constants and the experimental data. The experimental data are taken from single pulse shock tube studies performed recently in this laboratory.[6,7] As can be seen, the agreement is very good.

V. Conclusions

The isomerizations of dihydrobenzofuran and isodihydrobenzofuran can be summarized by following features.

(1) Both reactions proceed via stepwise mechanisms. The potential energy surface of dihydrobenzofuran → *o*-hydroxystyrene isomerization contains one intermediate and two transition states. In isodihydrobenzofuran → *o*-tolualdehyde isomerization, there are two intermediates and three transition states on the surface. A stable intermediate is produced in the dihydrobenzofuran isomerization because C−O bond breaking is accompanied by a 1,2-H-atom shift that brings about single- and double-bond rearrangements. In isodihydrobenzofuran, the intermediates are unstable biradicals. The last step in both isomerizations is an H-atom migration.

(2) The intermediate, methyl-2-methylene-3,5-cyclohexadiene-1-one, that is formed in the dihydrobenzofuran isomerization is very stable despite the complete loss of resonance energy of the benzene ring in the process. This was proven to be due to the formation of a very strong >C═O bond.

(3) Rate constants based on the quantum chemical calculations using transition-state theory are in very good agreement with the experimental results.

Acknowledgment. This research was supported by Grant No. 34/01-12.5 from the Israel Science Foundation (ISF), Jerusalem, Israel.

References and Notes

(1) Unsworth, J. F. *Coal Quality and Combustion Performance*; Elsevier Science Publishers: Amsterdam, 1991; p 206.
(2) Laskin, A.; Lifshitz, A. *Proc. Combust. Inst.* **1999**, *27*, 313.
(3) Laskin, A.; Lifshitz, A. *J. Phys. Chem. A* **1997**, *101*, 7787.
(4) Laskin, A.; Lifshitz, A. *J. Phys. Chem. A* **1998**, *102*, 928.
(5) Lifshitz, A.; Bidani, M. *J. Phys. Chem.* **1989**, *93*, 1139.
(6) Lifshitz, A.; Suslensky, A.; Tamburu, C. *Proc. Combust. Inst.* **2000**, *28*, 1733.
(7) Lifshitz, A.; Suslensky, A.; Tamburu, C. *J. Phys. Chem. A* **2001**, *105*, 3148.
(8) Wellington, C. A.; Walters, W. D. *J. Am. Chem. Soc.* **1961**, *83*, 4888.
(9) Rubin, J. A.; Filseth, S. V. *J. Chem. Educ.* **1969**, *46*, 57.
(10) Lifshitz, A.; Bidani, M.; Bidani, S. *J. Phys. Chem.* **1986**, *90*, 6011.
(11) Becke, A. D. *J. Chem. Phys.* **1993**, *98*, 5648.
(12) Lee, C.; Yang, W.; Parr, R. G. *Phys. Rev.* **1988**, *B37*, 785.
(13) . Dunning, T. H., Jr. *J. Chem. Phys.* **1989**, *90*, 107.
(14) Schlegel, H. B. *J. Comput. Chem.* **1982**, *3*, 214.
(15) Peng, C.; Schlegel, H. B. *Isr. J. Chem.* **1993**, *33*, 449.
(16) Skancke, P. N.; Hrovat, D. A.; Borden, W. T. *J. Phys. Chem. A* **1999**, *103*, 4043.
(17) Hess, B. A., Jr.; Eckart, U.; Fabian, J. *J. Am. Chem. Soc.* **1998**, *120*, 12310.
(18) Brinck, T.; Lee, H.-N.; Jonsson, M. *J. Phys. Chem. A* **1999**, *103*, 7094.
(19) Lee, T. J.; Taylor, P. R. *Int. J. Quantum Chem. Symp.* **1989**, *23*, 199.
(20) Lee, T. J.; Rendell, A. P.; Taylor, P. R. *J. Phys. Chem.* **1990**, *94*, 5463.
(21) Bartlett, R. J. *J. Phys. Chem.* **1989**, *93*, 1697.
(22) Cramer, C. J.; Nash, J. J.; Squires, R. R. *Chem. Phys. Lett.* **1997**, *277*, 311.
(23) Kraka, E.; Cremer, D. *J. Am. Chem. Soc.* **1994**, *116*, 4929.
(24) Frisch, M. J.; Trucks, G. W.; Schlegel, H. B.; Scuseria, G. E.; Robb, M. A.; Cheeseman, J. R.; Zakrzewski, V. G.; Montgomery, J. A., Jr.; Stratmann, R. E.; Burant, J. C.; Dapprich, S.; Millam, J. M.; Daniels, A. D.; Kudin, K. N.; Strain, M. C.; Farkas, O.; Tomasi, J.; Barone, V.; Cossi, M.; Cammi, R.; Mennucci, B.; Pomelli, C.; Adamo, C.; Clifford, S.; Ochterski, J.; Petersson, G. A.; Ayala, P. Y.; Cui, Q.; Morokuma, K.; Malick, D. K.; Rabuck, A. D.; Raghavachari, K.; Foresman, J. B.; Cioslowski, J.; Ortiz, J. V.; Stefanov, B. B.; Liu, G.; Liashenko, A.; Piskorz, P.; Komaromi, I.; Gomperts, R.; Martin, R. L.; Fox, D. J.; Keith, T.; Al-Laham, M. A.; Peng, C. Y.; Nanayakkara, A.; Gonzalez, C.; Challacombe, M.; Gill, P. M. W.; Johnson, B. G.; Chen, W.; Wong, M. W.; Andres, J. L.; Head-Gordon, M.; Replogle, E. S.; Pople, J. A. *Gaussian 98*, revision A.7; Gaussian, Inc.: Pittsburgh, PA, 1998.
(25) Dubnikova, F.; Lifshitz, A. *J. Phys. Chem. A* **2002**, *106*, 1026.
(26) Eyring, H. *J. Chem. Phys*. **1935**, *3*, 107.
(27) Evans, M. G.; Polanyi, M. *Trans. Faraday Soc*. **1935**, *31*, 875.
(28) Wigner, E. *Z. Phys. Chem.* **1932**, *B19*, 203.
(29) Louis, F.; Gonzales, C. A.; Huie, R.; Kurylo, M. J. *J. Phys. Chem. A* **2000**, *104*, 8773.
(30) George, P.; Glusker, J. P.; Bock, W. *J. Phys. Chem. A* **2000**, *104*, 11347.
(31) Kiefer, J. H.; Shah, J. N. *J. Phys. Chem.* **1987**, *91*, 3024.